# Iris Localization Based on Integro-Differential Operator for Unconstrained Infrared Iris Images

Vineet Kumar, Abhijit Asati, Anu Gupta
Department of Electrical and Electronics Engineering
Birla Institute of Technology and Science Pilani, Pilani Campus, India-333031
{vineet, abhijit_asati, anug}@pilani.bits-pilani.ac.in

***Abstract*—Iris localization is an important step for high accuracy iris recognition systems and it becomes difficult for iris images captured in unconstrained environments. The proposed method localizes irises in unconstrained infrared iris images having non-ideal issues such as severe reflections, eyeglasses, low contrast, low illumination and occlusions by eyebrow hair, eyelids and eyelashes. In the proposed method, the iris image is first preprocessed using morphological operation to remove reflections and make it suitable for subsequent steps. The proposed method detects pupil using Daugman's integro-differential operator (IDO) and iris's outer boundary is detected using proposed modified Daugman's IDO. The proposed method proposes a technique based on thresholding and morphological operation to reduce the number of pixels on which the IDO is applied for detecting pupil which improves the time performance and accuracy as well. The method was tested with CASIA-Iris-Thousand, version 4.0 (CITHV4) iris database which contains challenging images having non-ideal issues as described before. The average accuracy of the proposed method is 99.3% and average time cost per image is 1.86 seconds for CITHV4. The proposed method shows improvement in both accuracy and time when compared with some published state-of-the-art iris localization methods in the literature.**

***Keywords—Iris localization; Iris segmentation; Integro-differential operator; Iris recognition.***

## I. INTRODUCTION

Iris recognition offers high accuracy in security applications such as secured access to bank accounts at ATM machines, national border controls, secured access to buildings and passports control etc. [1]. An iris recognition system [2,3,4] typically contains four stages: iris localization, iris normalization, feature extraction and template matching. The iris localization is process of localizing iris's inner and outer boundaries. The iris localization is an important step because inaccurate iris localization may result in different representation of the iris patterns and such difference could cause recognition failure [2]. Iris localization algorithm takes input as an iris (eye) image from image acquisition system [4]. The iris images are captured under near infrared (NIR) illuminations or visible wavelength (VW) light. Most of the existing iris databases available for research purpose are NIR databases because irises show rich and complex features in NIR light [3]. The iris images collected in controlled environments are better inputs for iris recognition algorithms but the images captured in unconstrained environments may have different non-ideal issues such as lighting and specular reflections, eyeglasses, low contrast, low illuminations and occlusions by eyebrows hair, eyelids and eyelashes [1] as shown in Fig. 1. The unconstrained images complicate iris localization process.

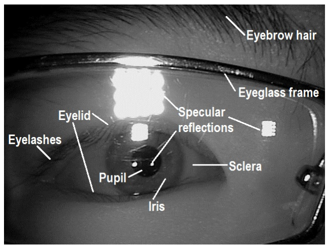


**Fig. 1.** Unconstrained infrared iris image ([13])

Most of the deployed and commercially available iris recognition systems are typically using Daugman's [3] and/or Wildes' [4] algorithms based iris localization. But the algorithms in [3,4] work under very controlled conditions and their performance deteriorates while dealing with the images having non-ideal issues as discussed previously. Some other published state-of-the-art iris localization methods are given in [5-12] which localize irises in ideal and/or non-ideal images.

The proposed method presented in this paper localizes irises in the unconstrained frontal view NIR iris images. In the proposed method, image is preprocessed first to counter some of non-ideal issues present in the image. Iris's inner boundary is localized by applying Daugman's IDO on selected pixels in the preprocessed image. The selected pixels are identified using the image thresholding and morphological operation on binary image. Iris's outer boundary is detected using proposed IDO which is a variant of Daugman's IDO. The method was implemented in MATLAB and tested with CASIA-Iris-Thousand, version 4.0 (CITHV4) iris database [13] which contains NIR images having non-ideal issues as described previously. The sample of unconstrained iris images from CITHV4 are shown later in section IV of the paper.

Remainder of this paper is organized as follows: Related Daugman's IDO approach is discussed in Section II and implementation of the proposed iris localization method is explained in section III. Section IV explains experimental results and discussion. Work is concluded in section V.

## II. RELATED DAUGMAN'S IDO APPROACH

The review of iris localization methods in the relevant literature reveals that there are two major approaches: Daugman's IDO and Hough transform based. As the proposed method in this paper uses Daugman's IDO as a circular edge detector, so, Daugman's IDO approach is discussed in this section. The first successful iris localization method was proposed by Daugman in 1993 which uses IDO (1) [3]. Daugman's IDO (1) was used to localize iris which considers iris's inner and outer boundaries as two circles inside iris image [2,3]. He applied the IDO (1) to the image domain to search for iris's outer boundary first then within the iris's outer boundary to search for pupil [3]. Daugman applied it on the images in which gray difference between iris and sclera is more than pupil and iris [3]. This is true for images captured under VW light. Given a pre-processed image, $I(x,y)$, the IDO (1) can be used first to determine the iris's outer boundary. Daugman's IDO (1) is mathematically expressed as below [3].

$$\max_{(r,x_o,y_o)} \left| G_\sigma(r) * \frac{\partial}{\partial r} \oint_{r,x_o,y_o} \frac{I(x,y)}{2\pi r} ds \right| \qquad (1)$$

The operator searches over image domain *(x,y)* for maximum in the blurred partial derivative with respect to increasing radius $r$ of the normalized contour integral of $I(x,y)$ along a circular arc $ds$ of radius $r$ and center coordinates ($x_o$, $y_o$) [3]. The symbol * denotes the convolution operation and $G_\sigma(r)$ is a smoothing function such as a Gaussian of scale $\sigma$ (standard deviation) [3]. To normalize the circular integral with respect to its perimeter, it is divided by $2\pi r$. In short, the IDO (1) behaves as circular edge detector blurred at a scale set by $\sigma$, which searches iteratively over image space through the parameter set {$x_o$, $y_o$, r} [3]. First search is for iris's outer boundary with higher value of $\sigma$ [3]. Once the iris's outer boundary is localized, the search process with finer value of $\sigma$, for the iris inner boundary is carried out only within the pre-determined region [3]. The computation time associated with an iris's outer boundary search process can be reduced by providing a range of estimates for the parameter $r$, that are close to the actual boundary radius.

## III. The Proposed Iris Localization Method

The pupil is localized prior to iris's outer boundary because pupil contour is stronger than iris's outer boundary in NIR iris images. The proposed method considers iris's inner and outer boundaries as perfect circles which is true for frontal view iris images. The iris localization is achieved in three phases. In first phase, iris image is preprocessed to counter some of the non-ideal image issues and make it suitable for subsequent steps. In second and third phase, iris's inner and iris's outer boundaries are localized respectively. The steps involved in the proposed iris localization method are shown in Fig. 2. The steps are discussed in three phases of the method below.

### *A. Image preprocessing*

The way IDO (1) works, it cannot be tolerant to reflection spots and uneven high intensity pixels present in the iris image. The reflection spots in iris images cover portions of the image that causes hindrance in the iris detection process. The original pixel intensity values are replaced by the much higher intensity values in the parts of the image, affected by light reflections as shown in Fig. 3(a). Therefore, the original information of these parts of the image has been lost. As apparent from Fig. 1 and Fig. 3(a), there is much difference in intensity values between reflection spots and surrounding dark pixels. In order to avoid light reflection and uneven high intensity pixel values affecting the iris detection, a morphological operator is used which fills

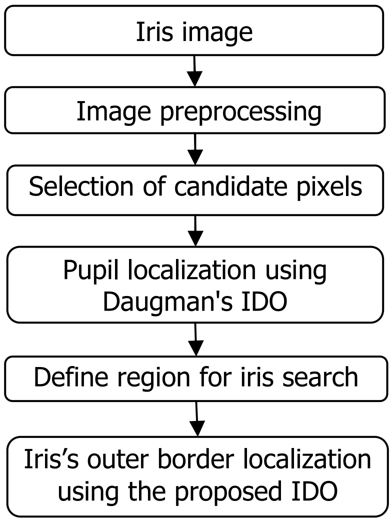


**Fig. 2.** Steps involved in the proposed iris localization method

in the high intensity regions with the average of intensities of pixels from the region surrounding them. The MATLAB function 'imfill' with hole filling option available in [14] is used as the morphological operator which is applied on the complemented iris image. Taking the complement again, returns the original iris image in which reflection spots and high intensity pixels are removed as shown in Fig. 3(b). The image shown in Fig. 3(b) is called preprocessed iris image which is used as input image for both iris's inner and outer boundary localization.

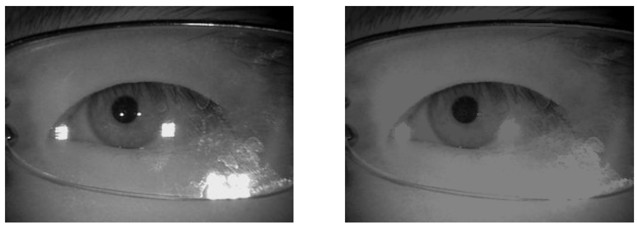

(a) (b)

**Fig. 3.** Image preprocessing: **(a)** A noisy image from CITHV4 [13]; **(b)** The preprocessed iris image obtained from (a).

### *B. Iris's inner boundary (pupil) localization*

To localize pupil using IDO (1), the image pixels on which the IDO is applied are identified first otherwise it may take much large time in localizing pupil. These identified pixels are the potential centers of pupil circle (pupil-centers). The inputs given to the IDO (1) for pupil localization are a range of pupil radii ($rmin_p$ to $rmax_p$) and a set of image pixels which are the potential pupil-centers. The set of image pixels on which the IDO (1) is applied are obtained using the steps below which reduces the false candidate pixels those cannot be potential pupil-centers. Pupil localization steps are shown in Fig. 4.

*1) Image binarization:* The pupil pixels are obtained from the iris image using thresholding operation [15] as pupil is relatively much darker region as compared with the iris, sclera and the skin. The global thresholding is used in which appropriate threshold intensity value is selected using the iris

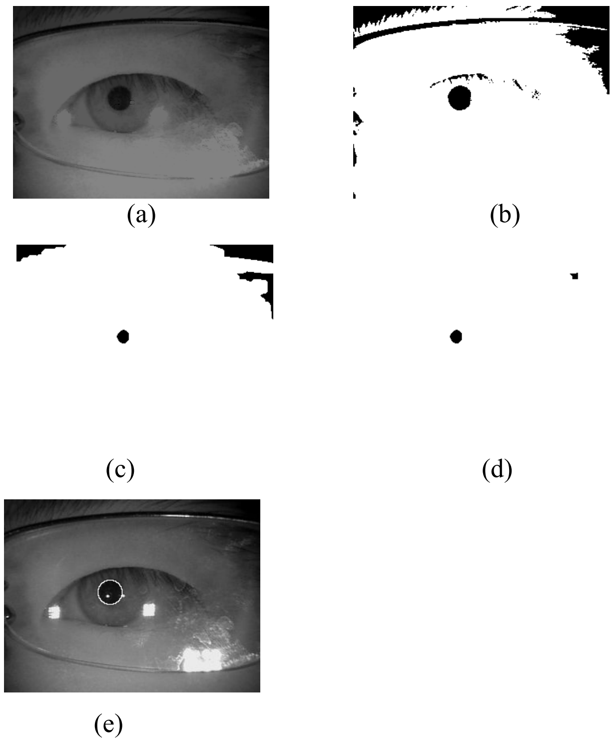


**Fig. 4.** Pupil localization in the proposed method: **(a)** Preprocessed iris image; **(b)** Binarized-image obtained after thresholding (a); **(c)** Binary image after image cleanup on (b); **(d)** After removing pixels close to image border in (c); **(e)** Pupil localized image using IDO (1) .

image histogram [16]. The thresholding operation on an intensity image f(x,y) with global threshold T results in binary image g(x,y).

$$g(x,y) = \begin{cases} 1 & \text{if } f(x,y) \geq T \\ 0 & \text{otherwise} \end{cases}$$

The T value is selected once for whole iris database and do not need to be computed for each iris image. The binary iris image, shown in Fig. 4(b), is obtained by applying thresholding on the preprocessed iris image of Fig. 4(a). The black regions in the binary iris image (see Fig. 4(b)) correspond to pupil, eyelashes, eyelids, eyeglass frame and low illumination near the image border. The regions other than pupil in the image are noise and are false candidate pixels for pupil-center. So, they are removed using morphological operation below.

*2) Binary Image cleanup:* The noise in the binarized-image is removed using image erosion for black objects which is a morphological operation [15]. The erosion operation uses a structuring element of type disk because pupil is circular region [15]. The disk radius value must be smaller than the minimum pupil radius in the selected iris image database. The disk radius is taken as 15 for CITHV4. A larger disk radius value may remove pupil completely and a smaller value may not remove false candidate pixels significantly. The image after erosion operation is shown in Fig. 4(c) which removes the noise to a much extent and reduces pupil size also. This step not only reduces false candidate pixels for pupil-center due to noise but also removes pixels in the pupil which cannot be potential pupil-center pixels. The false candidate pixels are further reduced using step below.

*3) Removing pixels close to image border:* It is certain in every iris image that pupil cannot be touching the image border as pupil is surrounded by iris region. So, some pixels closer to the image border can be discarded as they cannot be potential pupil-centers. The range (distance) of discarded pixels from image border is taken as $\{k \times rmin_p\}$, where the k is a positive scalar greater than one whose value is estimated by visualizing the iris database images. The value of k chosen for CITHV4 is 3.5 and $rmin_p$ is equal to 20. The value of k depends on the database chosen. The remaining pixels after removing the pixels close to border are shown in Fig. 4(d). The black pixels in Fig. 4(d) are identified as potential pupil-centers.

The reduced candidate pixels as a result of above discussed steps are identified as potential pupil-centers. Now, the IDO (1) discussed in section II of the paper is applied on set of reduced candidate pixels' coordinates in the preprocessed iris image which gives center and radius of pupil as output.

### *C. Iris's outer boundary localization*

Iris's outer boundary localization may be hurdled by eyelids, eyelashes, reflections and low contrast between the iris and sclera. The reflections and uneven high intensity values have already been removed after the image preprocessing step. The eyelids and eyelashes occlusion as shown in Fig. 5 is handled by IDO (2) which acts as arc detector and it has been derived by taking motivation from Daugman's IDO (1).

The IDO (2) for iris's outer boundary localization is mathematically expressed as:

$$\max_{(r,x_o,y_o)} \left| G_\sigma(r) * \left[ \frac{\partial}{\partial r} \left( \int_{-\pi/4}^{\pi/6} \frac{I(x,y)}{5\pi r/12} ds + \int_{5\pi/6}^{5\pi/4} \frac{I(x,y)}{5\pi r/12} ds \right) \right] \right| \quad (2)$$

The parameter *r* denotes the radius of the circular arc *ds* centered at $(x_o, y_o)$. To normalize the arc-pixels' intensities integral with respect to arc length, it is divided by $5\pi r/12$.The IDO (2) searches iteratively over a portion of the image domain for the maximum difference of sum of contour pixels intensities between two adjacent circular arcs one pixel radius apart and defined by {–π/4: π/6 and 5π/6: 5π/4} rad (see Fig. 5).

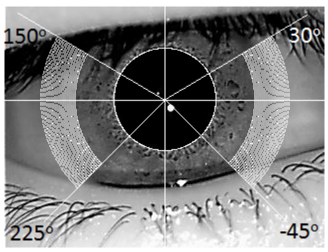


**Fig. 5.** Selection of iris search region in the image.

Fig. 5 shows that iris may be occluded by upper and/or lower eyelids and eyelashes in the iris images. So, upper and lower parts of iris contour may not be visible but left and right parts are always visible [10] which is used as the input information to the IDO (2).

*1) Define iris search region:* The iris search area is defined by the pupil center, radii range of the iris's outer boundary and a small area around pupil-center which contains potential candidate pixels for centers of iris's outer boundary circle. The white area on both sides of pupil in Fig. 5 represents search region for the proposed IDO (2) with $(x_o, y_o)$ equal to pupil center. As the pupil and iris's outer contour circles may not be concentric [2], the IDO (2) is applied on a rectangle of size $10 \times 10$ centered at pupil center to find precise center and radius of iris's outer boundary circle. Iris localized iris image is shown in Fig. 6(b).

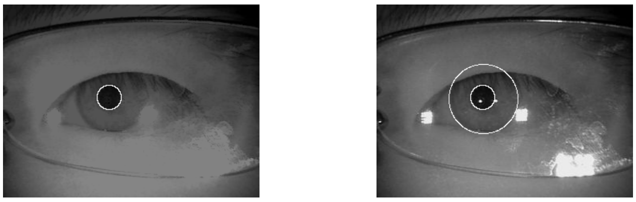

(a) (b)

**Fig. 6.** Iris's outer boundary localization: **(a)** Inputs are preprocessed iris image with pupul center known; **(b)** Iris localized image obtained using IDO (2)

## IV. EXPERIMENTAL RESULTS AND DISCUSSION

To evaluate performance of the proposed method, we used MATLAB version 8.3 installed on a PC with Windows 7 Professional, Intel® Core™ i5 CPU @ 2.40 GHz, 8.00 GB RAM and a set of images from CITHV4 [13].

### *A. Input dataset*

The short description of iris database [13] taken for testing the proposed method is given below.

- CITHV4 contains 20000 iris images collected from 1000 subjects. The main sources of intra-class variations in the database are eyeglasses and specular reflections [13]. CITHV4 images are 8-bit gray-level JPEG files with resolution 640×480 pixel and collected under near infrared illumination [13]. The CASIA-Iris-Thousand is the first publicly available iris dataset with one thousand subjects. The detailed description is available at [13]. Collectively, the images in the database contain non-ideal issues such as occlusions by eyelids, eyelashes, eyebrow hair, eyeglasses, low illumination, low contrast and reflections.

The first 1000 images from CASIA Iris-Thousand V4.0 were taken for testing the proposed method.

### *B. Results and discussion*

Fig. 7 shows sample of unconstrained images from the CITHV4 in which accurately localized irises by the proposed method are shown.

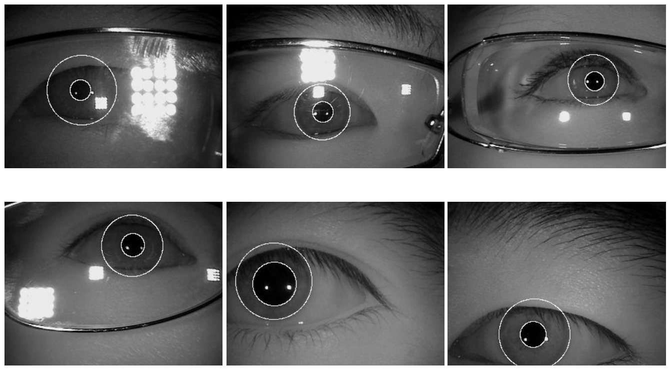

**Fig. 7.** Accurately localized irises using the proposed method from CITHV4 [13].

The percentage accuracy of a localization method is defined as [16]:

$$\text{Accuracy (\%)} = \frac{N_I}{N_T} \times 100$$

where $N_I$ is number of irises accurately localized and $N_T$ is total number of iris images taken for testing. To find the average time cost per image, first 1000 images from the CITHV4 were taken. MATLAB timer functions 'tic' and 'toc' were used to find execution time of a code which runs to localize 1000 images and dividing the execution time by 1000 gives average time cost per image. The experimental results of the proposed localization method are shown in Table I.

TABLE I. EXPERIMENTAL RESULTS

| Iris Database | Accuracy (%) & Average time cost per image (sec) | |
|---|---|---|
| | *Proposed method* | *L. Masek method [17]* |
| CITHV4* (640×480) | **99.3 & 1.86** | 84 & 5.52 |

*CITHV4: CASIA-Iris-Thousand, version 4.0

For the same database images, we also tested L. Masek's iris localization method which is an edge detection and Hough transform based algorithm whose open source code in MATLAB is available on web at [17] and results of testing are shown in Table I. Table I shows that the proposed method has much better results than L. Masek method [17].

To compare the proposed method with published iris localization methods in the literature, we chose Jan et al. [9,16] work because their iris localization methods were tested with the CITHV4 which we have used for testing the proposed method. Also, Jan et al. [9,16] are highly accurate methods in the literature as described in Jan et al. [9]. Table II shows that accuracy of the proposed method is similar to Jan et al. [9,16] but time cost performance is much better than Jan et al. [9,16] methods. The major reason of reduced time cost of the proposed method is reduced number of pixels on which IDO (1) is applied during pupil localization. The use of IDO (2) also reduces time cost of iris localization.

To compare the proposed method with Daugman's algorithm [2] and other famous published methods in the literature [12,18], we also tested the proposed method with

MMU V1.0 iris database [19] because testing results for CITHV4 were not found in the literature. Table III shows that the accuracy of the proposed method for MMU V1.0 is 99.11% which is better than some state-of-the-art published methods [2,12,18]. The proposed method has average time cost of 0.67 seconds per image for MMU V1.0.

We also implemented Daugman's algorithm described in [2] which uses the IDO (1) to localize both boundaries of iris and obtained accuracy of 93% for MMU V1.0. The use of IDO (2) to localize iris's outer boundary is major reason for improvement in the accuracy of proposed method as compared to Daugman's algorithm [2]. The reduction in the number of false candidate pixels that cannot be potential centers of pupil circle is another factor that makes proposed method more accurate.

TABLE II. COMPARISON OF ACCURACY AND TIME COST WITH PUBLISHED IRIS LOCALIZATION METHODS

| **Method** | **CITHV4*** | |
|---|---|---|
| | ***Accuracy (%)*** | ***Time cost per image (sec)*** |
| Jan et al. [9] | 99.5 | 4.93 |
| Jan et al. [16] | 99.23 | 3.4 |
| **Proposed method** | **99.3** | **1.86** |

*CITHV4: CASIA-Iris-Thousand, version 4.0

TABLE III. COMPARISON OF ACCURACY WITH PUBLISHED RESULTS (Accuracy results in the table are taken from [20])

| **Method** | **Accuracy (%) for MMU V1.0** |
|---|---|
| Daugman [2] | 85.64 |
| Ma et al.[18] | 91.02 |
| Daugman (new)[12] | 98.23 |
| **Proposed method** | **99.11** |

## V. CONCLUSIONS

In this paper, we have presented a method to localize irises in unconstrained NIR iris images. The proposed method starts with image preprocessing followed by iris's inner and outer boundary detection using Daugman's IDO and the proposed modified Daugman's IDO respectively. A novel technique in pupil localization is proposed to reduce the number of false candidate pixels which cannot be potential centers of pupil circle. Also, the method proposes modified Daugman's IDO to detect iris's outer boundary. The introduction of above mentioned techniques enhance the time and accuracy performance of iris localization based on the IDO as demonstrated by testing results of the proposed method. The experimental results show that the proposed method is highly accurate and is tolerant to non-ideal issues in iris images such reflections, eye-glasses, low contrast, low illumination and occlusions by eyelids, eyelashes and eyebrow hair. The comparison of the proposed method with published work in the literature shows it outperforms on some state-of-the-art iris localization methods in both accuracy and computation time.

## ACKNOWLEDGMENT

Portions of the research in this paper use the CASIA-IrisV4 collected by the Chinese Academy of Sciences' Institute of Automation (CASIA). We thankfully acknowledge CASIA for providing us the iris images. We also thank Multimedia University for providing MMU V1.0.

## REFERENCES

[1] F. Jan, I. Usman, S.A. Khan, S.A. Malik, "A dynamic non-circular iris localization technique for non-ideal data", Comput. Electr. Eng., 2014, http://dx.doi.org/10.1016/j.compeleceng.2014.05.004.

[2] J. Daugman, "How iris recognition works", IEEE Trans. Circuits Syst. Video Technol., 14, (1), pp. 21–30, 2004.

[3] J. Daugman, "High Confidence visual recognition of persons by a test of statistical independence", IEEE Trans. Pattern Anal. Mach. Intell., vol. 15, no. 11, pp. 1148–1160, Nov. 1993.

[4] R.P. Wildes, "Iris recognition: An emerging biometric technology", Proc. IEEE, vol. 85, no. 9, pp. 1348–1363, Sep. 1997.

[5] Z. He, T. Tan, Z. Sun, and X. Qiu, "Toward accurate and fast iris segmentation for iris biometrics", IEEE Trans. Pattern Anal. Mach. Intell., vol. 31, no. 9, pp. 1670–1684, Jul. 2009.

[6] Y. Chen, M. Adjouadi, C. Han et al., "A highly accurate and computationally efficient approach for unconstrained iris segmentation", Image Vis. Comput., 28, (2), pp. 261–269, 2010.

[7] T. Tan, Z. He, Z. Sun, "Efficient and robust segmentation of noisy iris images for non-cooperative iris recognition", Image Vis. Comput., 28, (2), pp. 223–230, 2010.

[8] N.B. Puhan, N. Sudha, A. Sivaraman Kaushalram, "Efficient segmentation technique for noisy frontal view iris images using Fourier spectral density", Signal Image Video Process., 5, (1), pp. 105–119, 2011.

[9] F. Jan, I. Usman, S. Agha, "Iris localization in frontal eye images for less constrained iris recognition systems", Digit. Signal Process., 22, (6), pp. 971–986, 2012.

[10] A. Radman, "Fast and reliable iris segmentation algorithm", IET Image Processing, 7(1), pp.42-49, 2013.

[11] K. Grabowski, W. Sankowski, M. Zubert, M. Napieralska, "Reliable iris localization method with application to iris recognition in near infrared light", MIXDES, Proceedings of the International Conference, June 22-24,pp.684-687, 2006.

[12] J. Daugman, New methods in iris recognition, IEEE Trans. Syst. Man Cybern. B, Cybern., 2007, 37, (5), pp. 1167–1175.

[13] CASIA Iris Image Database, 2010, Chinese Academy of Sciences' Institute of Automation. Available: http://biometrics.idealtest.org/.

[14] The MATLAB (version 8.3) function 'imfill' description, 2014. Available: http://in.mathworks.com/help/images/ref/imfill.html.

[15] R.C. Gonzalez, R.E. Woods, S.L. Eddins, Digital Image Processing Using MATLAB, Gatesmark Publishing, 2009.

[16] F. Jan, I. Usman, S. Agha, "Reliable iris localization using Hough transform, histogram-bisection, and eccentricity", Signal Processing, 93(1), pp. 230–241, 2013.

[17] L. Masek, P. Kovesi, "MATLAB source code for a biometric identification system based on iris patterns", The School of Computer Science and Software Engineering, The University of Western Australia, 2003. Available: http://www.csse.uwa.edu.au/~pk/studentprojects/libor/sourcecode.html.

[18] L. Ma, T. Tan, Y. Wang, D. Zhang, "Local intensity variation analysis for iris recognition", Pattern Recognition, vol. 37, Issue 6, pp. 1287–98, 2004

[19] MMU Iris Image Database, 2004, Multimedia University. Available: http://pesona. mmu.edu. my/~ccteo/.

[20] M.T. Ibrahim, T.M. Khan, S.A. Khan, M.A. Khan, L. Guan, "Iris localization using local histogram and other image statistics", Opt. Lasers Eng., 50, (5), pp. 645–654, 2012.